

Prognosis and immune infiltration analysis of SASP-related genes in bladder cancer

YAXuan Wang

Nantong University

Xiaolin Wang (✉ cxhwyc2010@163.com)

HaiXia Zhu

Nantong Tumor Hospital

Kun Zhang

Nantong University

Research

Keywords: SASP, Prognosis, Immunity, Prognostic markers, BLCA

Posted Date: May 24th, 2022

DOI: <https://doi.org/10.21203/rs.3.rs-1660686/v1>

License:   This work is licensed under a Creative Commons Attribution 4.0 International License.

[Read Full License](#)

Abstract

Background: Bladder Urothelial Carcinoma (BLCA) is one of the most common tumors of the male urinary system. It is highly heterogeneous and there is still a lack of biomarkers to predict prognosis in patients with advanced BLCA. Senescence-associated secretory phenotype (SASP) plays an important role in tumor and many studies have shown that it is closely related to the immune microenvironment. The aim of this study was to investigate the prognostic value of SASP-related genes and BLCA immune infiltration.

Results: There were significant differences in the expression of SASP-related genes in BLCA. Functional enrichment analysis revealed that the 18 SASP-related genes were mainly related to the "HIF-1 signaling pathway", "PI3K-Akt signaling pathway", and "IL-17 signaling pathway". A SASP-related gene signature stratifying patients into 2 risk score groups was established based on the TCGA cohort. Patients with higher risk scores had worse overall survival. In addition, we also found that SASP-related genes were closely related to immune cell infiltration.

Conclusions: In conclusion, our study confirms the influence of SASP-related genes in BLCA on the prognostic value and immune microenvironment. This will provide important evidence for future research on the role of SASP in BLCA.

Background

Cancer is the leading cause of death in countries around the world and an important barrier to improving life expectancy [1]. Bladder cancer, as one of the three major tumors of the urinary system, is one of the top ten tumors with the highest incidence, with 573,000 new cases in 2020 [2]. Bladder cancer has traditionally been classified as non-invasive bladder cancer (NMIBC) or muscle-invasive bladder cancer (MIBC). NMIBC is the most common and has the highest recurrence rate, and MIBC has a high rate of metastasis and mortality [3]. Chemotherapy, immunotherapy and targeted therapy are the preferred treatments for patients with advanced bladder cancer. However, treatment outcomes in patients with advanced bladder cancer have been unsatisfactory due to drug resistance, individual differences, and a lack of reliable prognostic biomarkers. Studies have shown that BLCA patients benefit significantly from adjuvant chemotherapy and new immune checkpoint inhibitors (ICIs) [4]. However, due to tumor immune evasion, a significant proportion of patients do not respond to immunotherapy at all stages of BLCA [5]. Therefore, it is important to study the immune microenvironment of bladder tumor and to find effective biomarkers that can be used to identify and predict the survival of bladder patients.

Senescence has long been known as a tumor suppressor mechanism. However, paracrine signaling in senescent cells has recently attracted attention for its pro-tumor role. Senescence is a damage-induced stress process that activates a range of cytokines, chemokines, growth factors, and age-related secretory phenotypes (SASP) proteases. Finally, it leads to the permanent suppression of tumor cells and the remodeling of tumor immune microenvironment [6]. Therefore, changes in secretion and surface

composition of senescent cells provide research directions for existing and new immunotherapy strategies.

The prognostic value of SASP-related genes in bladder cancer and the relationship between SASP-related genes and immune microenvironment have not been clarified. The present study analyzed the expression, prognosis and immune invasion of SASP-related genes in bladder cancer. We also clustered subtypes according to the expression level of SASP-related genes. Therefore, there is significant tumor heterogeneity, different PD-L1 expression and tumor immune microenvironment between the two subtypes, promoting risk stratification and precision therapy for bladder cancer patients. In addition, the establishment of a prognostic model of SASP-related genes is expected to provide a basis for searching for prognostic biomarkers and therapeutic targets of bladder cancer. Finally, HLA-G was identified as a key gene in a potential immune-infiltration-related SASP, and we analyzed the association between HLA-G and immune cell biomarkers, Immunoinhibitors, Immunostimulators, and chemokines.

Materials And Methods

Data Acquisition

RNA-seq data and clinical information of the BLCA cohort were downloaded from the Genomic Data Commons (GDC) data portal of The Cancer Genome Atlas (TCGA) database (<https://portal.gdc.cancer.gov/>). Data included 19 normal kidney and 408 BLCA tissues.

Functional enrichment analysis

Kyoto Encyclopedia of Genes and Genomes(KEGG) analysis and Gene Ontology (GO) (including cellular component (CC),the biological process (BP), and molecular function (MF) categories) analysis were performed using the "GGplot2" package in R software.

Consensus Clustering Analysis

RNA-sequencing expression (level 3) profiles and corresponding clinical information for BLCA were downloaded from the TCGA dataset(<https://portal.gdc.com>). Consistency analysis by using ConsensusClusterPlus R package (v1.54.0), the maximum number of clusters is 6, and 80% of the total sample is drawn 100 times, clusterAlg = "hc", innerLinkage='ward.D2'. Use the R software package pheatmap (v1.0.12) for clustering heatmaps.

Establishment of a prognostic model of SASP-related genes in BLCA

RNA-sequencing expression (level 3) profiles and corresponding clinical information for BLCA were downloaded from the TCGA dataset. Converting counts data to TPM and normalizing the data \log_2 (TPM+1), keeping samples with clinical information at the same time. Finally there are BLCA samples for subsequent analysis. Log-rank test was used to compare differences in survival between these groups. The timeROC (v 0.4) analysis was used to compare the predictive accuracy of BLCA gene and risk score.

Lasso: The least absolute shrinkage and selection operator (LASSO) regression algorithm was used for feature selection, 10-fold cross-validation was used, and the R package glmnet was used for the analysis. For Kaplan-Meier curves, p-values and hazard ratio (HR) with 95% confidence interval (CI) were generated by log-rank tests and univariate cox proportional hazards regression. All the analysis methods and R packages were implemented by R (foundation for statistical computing 2020) version 4.0.3. p value <0.05 was considered statistically significant.

Correlation analysis of SASP-related genes prognosis model and immune infiltration

The abscissa represents the distribution of the gene expression or the score, and the ordinate represents the distribution of the immune score. The density curve on the right represents the trend in distribution of the immune score, the upper density curve represents the trend in distribution of the gene expression or the score. The value on the top represents the correlation p value, correlation coefficient and correlation calculation method. Used Spearman's correlation analysis to describe the correlation between quantitative variables without a normal distribution. P values less than 0.05 were considered statistically significant (*P < 0.05).

Correlation analysis of SASP-related genes and immunostimulators, immunoinhibitors, chemokines, and receptors in BLCA

TISIDB (<http://cis.hku.hk/TISIDB/index.php>) was utilized to investigate the association of HLA-G with 45 immunostimulators, 24 immunoinhibitors, 41 chemokines, and 18 receptors in BLCA.

Result

SASP-related genes were screened in BLCA

We're from GenesCards to senescence in website (<https://www.genecards.org/>) associated secretory phenotype (SASP) for keywords, A total of 96 genes with SASP score > 7.0 were selected. *Then, the prognostic significance of these 96 genes in bladder cancer was analyzed, and 18 prognostic related genes were obtained (PPARG,PRKG1,NFKB1,GATA4,EGFR,CAV1,IGF1,SPINK1,HLA-G,IL4,VEGFA,CD36,MMP9,ACTA2,SRC,MAPK3,SERPINE1,ILK)(figure 1B). Of the 18 genes, PRKG1 NFKB1, CAV1, IGF1, CD36, ACTA2, ILK expression in bladder cancer is lower than the corresponding normal tissues. The expressions of HLA-G, MMP9 and SRC in bladder cancer were higher than those in the corresponding normal tissues, while there were no significant differences in the expressions of PPARG, GATA4,EGFR, SPINK1,IL4,VEGFA, MAPK3 and SERPINE1 in bladder cancer and the corresponding normal tissues(figure 1A). We also analyzed the associations of these 18 genes in bladder cancer samples from the TCGA database (figure 1C) And a grid of their interactions is drawn from STRING (<https://cn.string-db.org/>) (medium confidence 0.4)(figure 1D).*

Expression and prognostic significance of SASP-related genes in bladder cancer. A: Expression of 18 genes in bladder cancer. B: Prognostic forest map of 18 genes in bladder cancer. C:Correlation network

diagram of 18 genes in bladder cancer. D: Interaction network diagram of 18 genes.

SASP-related gene enrichment analysis

To elucidate the function of SASP-related genes in tumors, we analyzed these genes using KEGG and GO databases. KEGG enrichment analysis showed that SASP-related genes were significantly correlated with "HIF-1 Signaling Pathway", "PI3K-Akt Signaling Pathway", and "IL-17 Signaling Pathway", and bladder cancer (figure 2A). The important roles of these three factors in tumor immune microenvironment have been reported [7][8][9]. GO enrichment analysis showed that SASP-related genes were most correlated with peptidyl-L-Tyrosine phosphorylation, membrane Raf and protein heterodimerization activity (figure 2B-D).

KEGG/GO analysis of SASP-related genes. A: KEGG pathway analysis. B: GO Biological Process. C: GO Cellular Component analysis. D: GO Molecular Function analysis.

Consensus Clustering Analysis of SASP Regulators Revealed Significant Differences in Baseline Characteristics and Survival Between Two Patient Clusters

ConsensusClusterPlus (v1.54.0) is used for consistency analysis. Based on the expression level of selected SASP-related genes and the proportion of fuzzy clustering measures, $k = 2$ was determined to be the best clustering stability from $K = 2$ to 6 (figure 3A-B). Subsequently, we analyzed the expression of SASP-related genes in these 2 clusters, and found that 11 genes were highly expressed in cluster 2, 4 genes were highly expressed in cluster 1, and 3 genes showed no significant difference between cluster 1 and cluster 2 (figure 3C-D). We also analyzed OS and PFS of clusters 1 and 2 in bladder cancer, and the results showed that cluster 2 was significantly associated with poor prognosis of BLADDER cancer OS and PFS (figure 3E-F). Subsequently, differences were noted in the clinicopathological characters and prognosis between the two subtypes, as shown in Table 1. There was no statistical significance between the two clusters except for age and sex ($P > 0.05$), and other pathological features were statistically significant.

Differential expression patterns and survival rates of SASP-related genes in two bladder cancer subtypes.

(A) $K = 2$ consensus clustering matrix. (B) The cumulative distribution function of $k = 2-6$. (C-D) Heat and box plots show the expression patterns of SASP-related genes in two bladder cancer subtypes. (E-F) Kaplan-meier curves showed OS (E) and PFS(F) in patients with bladder cancer in both groups. * $p < 0.05$ ** $p < 0.01$ *** $p < 0.001$.

Table 1 Clinical characteristics of two groups of patients with bladder cancer.

	Feature	Cluster 1	Cluster 2	P_value
Status	Alive	135	94	0
	Dead	71	108	
Age	Mean (SD)	67.4 (11.3)	68.8 (9.8)	0.161
	Median [MIN, MAX]	68 [34,90]	69 [43,90]	
Gender	FEMALE	50	57	0.428
	MALE	156	145	
Race	ASIAN	38	6	0
	BLACK	11	12	
	WHITE	149	175	
pT_stage	T1	7	4	0.001
	T2	70	40	
	T2a	21	11	
	T2b	25	24	
	T3	22	24	
	T3a	20	26	
	T3b	18	47	
	T4	1	7	
	T4a	18	15	
	T4b	1	1	
	TX	3	3	
pN_stage	N0	121	116	0.027
	N1	17	29	
	N2	34	41	
	N3	4	4	
	NX	26	10	
pM_stage	M0	120	76	0
	M1	5	6	
	MX	80	118	
pTNM_stage	I	2		0
	II	87	43	
	III	57	83	
	IV	58	76	
Grade	High Grade	184	200	0
	Low Grade	20	1	
	Unknown	2	1	

Association of SASP-related genes with genes related to immune cell infiltration and immunoassay sites in bladder cancer

In order to investigate the effect of SASP-related genes on the immune microenvironment of bladder cancer, TIMER and CIBERSORT methods were used to evaluate the relationship between cluster 2 and genes related to immune cells and immune examination sites. The classification of the two subtypes

based on expression levels of selected SASP-related genes revealed significant differences in immune cell infiltration (figure A-D). In addition, we also analyzed the relationship between cluster 2 and immunoassay sites, and the results showed that there were significant differences in the expression of genes related to immunoassay sites in cluster 2 (figure 4F). PD-L1 (CD274) plays an important role in the immunotherapy of bladder cancer. Therefore, we detailed the expression of PD-L1 in two clusters, and the results showed that the expression of PD-L1 in cluster 2 was significantly higher than that in cluster 1 ($P=3.1e-18$) (figure 4E). Therefore, we believe that SASP-related genes play an important role in the immune microenvironment of bladder cancer.

The differential infiltration level of tumor immune cells in two bladder cancer (BLCA) subtypes. A-D: The infiltrating levels of various immune cell types in two subtypes in the TCGA-BLCA cohort. E: PD-L1 expression was significantly different in 2 clusters. F: Heat maps of gene expression associated with two clusters of immunoassay sites. * $p < 0.05$, ** $p < 0.01$, *** $p < 0.001$, and **** $p < 0.0001$.

Construction of LASSO model

The LASSO Cox regression model was used to select the most predictive genes as prognostic indicators. λ was selected when the median of the sum of squared residuals was the smallest. Five potential predictors (figure 5A-B). MAPK3, SRC, CD36, VEGFA, IL4, HLA-G, SPINK1, IGF1, EGFR, GATA4, NFKB1, PRKG1 were identified as prognostic factors for BLCA. The risk score = $(0.1426) * PRKG1 + (-0.2351) * NFKB1 + (-0.0116) * GATA4 + (0.1326) * EGFR + (0.0676) * IGF1 + (-0.0303) * SPINK1 + (-0.1331) * HLA-G + (-0.043) * IL4 + (-0.02) * VEGFA + (0.0246) * CD36 + (-0.0326) * SRC + (0.1409) * MAPK3$. Patients with BLCA were divided into two groups based on risk score. The distribution of risk score, survival status and expression of these 12 genes are shown in Figure 5C. Kaplan-meier curves showed that patients with high risk BLCA had a lower overall survival rate than patients with low risk BLCA (median time = 1.8 and 5.3 years, $p = 4.77e-06$) (figure 5D). AUC in the 1-year, 3-year and 5-year ROC curves were 0.703, 0.682 and 0.673 respectively (figure 5E). These results suggest that SASP-related genes can be used as biomarkers for the prognosis of BLCA.

Genetic prognostic model of SASP-related genes. (A) Partial likelihood deviance versus $\log(\lambda)$ was drawn using LASSO Cox regression model. (B) Coefficients of selected features are shown by lambda parameter. (C) Distribution of risk score, survival status, and the expression of 12 prognostic SASP-related genes in BLCA. (D-E) Overall survival curves for BLCA patients in the high-/low-risk group and the ROC curve of measuring the predictive value.

Building a predictive nomogram

Considering the clinicopathologic features and these 12 prognostic SASP-related genes, we also built a predictive nomogram to predict the survival probability. Univariate and multivariate analyses showed that HLA-G, EGFR, CD36 expression, age and pTNM stage were independent factors affecting the prognosis of BLCA patients (figure 6A-B). The predictive nomogram suggested that the 3-year and 5-year overall survival rates could be predicted relatively well compared with an ideal model in the entire cohort (figure 6C-D).

Construction of a predictive nomogram. (A-B): The risk ratios and P values of the components involved in univariate and multivariate Cox regression for clinical parameters of BLCA and 12 SASP-related genes. (C-D): Nomogram to predict the 1, 3, and 5 year overall survival rate of BLCA patients. Calibration curve for the overall survival nomogram model in the discovery group. A dashed diagonal line represents the ideal nomogram.

Correlation analysis of SASP-related genes prognosis model and tumor immune infiltration in BLCA

SASP plays an important role in the development of tumor immune microenvironment. In this study, we also used TIMER and MCPOUNTER methods to analyze the correlation between SASP-related genes prognosis model and various immune cells. The results of TIMER method showed that B cell, T cell CD4+, T cell CD8+, Neutrophil, Macrophage and Myeloid dendritic cell was positively correlated with SASP-related genes prognosis model (figure 7A). SASP-related genes prognosis model was positively correlated with cytotoxicity score, NK cell, B cell, Macrophage/Monocyte, Myeloid dendritic cell, Endothelial cell by MCPOUNTER method (figure 7B).

Correlation analysis of SASP-related genes prognosis model and tumor immune infiltration. (A): TIMER method was used to analyze the correlation between SASP-related genes and immune infiltrating cells. (B): MCPOUNTER method was used to analyze the correlation between SASP-related genes and immune infiltrating cells.

Key SASP genes in BLCA were obtained by screening

PD-L1 plays an important role in immunotherapy of various tumors, including bladder cancer. Correlation analysis of PD-L1 with 12 SASP-related genes in BLCA prognostic model showed that PD-L1 was positively correlated with CD36, EGFR, HLA-G, IGF1, NFKB1, PRKG1, and negatively correlated with SPINK1, SRC, and VEGFA (figure 8A). Subsequently, we took the cross points of the gene set with high expression of SASP-related genes in bladder cancer, the gene set with positive correlation with PD-L1, and the gene set with significant difference in multivariate analysis of the genes in our prognostic model, we get a single gene—HLA-G (figure 8B). We also showed the correlation between PD-L1 and HLA-G in detail (correlation coefficient: 0.33, $P = 7.29E-12$, figure 8C). Sankey diagram showed the distribution trend of HLA-G expression on age, pTNM stage, grade and BLCA survival in TUMOR samples of BLCA (figure 8D). Finally, in bladder cancer, we grouped high HLA-G expression and low HLA-G expression into groups for KEGG enrichment analysis. The results showed that HLA-G expression was significantly correlated with 'Th1 and Th2 cell differentiation' and 'Th2 cell differentiation', suggesting that HLA-G plays an important role in tumor immune microenvironment.

HLA-G plays an important role in BLCA immune microenvironment. (A) Correlation analysis of PD-L1 and SASP related genes. (B) Venn diagram showed that HLA-G was up-regulated in bladder cancer, with significant difference in multivariate analysis and positive correlation with PD-L1. (C): Correlation analysis between PD-L1 and HLA-G. (D): The distribution trend of HLA-G expression and age, TNM grade in patients with bladder cancer. (E) KEGG enrichment analysis of HLA-G expression in BLCA.

Correlation Analysis of HLA-G Expression With Infiltrating Immune Cells

To identify a discrepancy in the TIME of BLCA patients with high and low expression levels of HLA-G, the TIMER and CIBERSORT algorithm was carried out to explore the difference of numerous immune cell subtypes between the HLA-G high expression group and the low expression group in BLCA. TIMER algorithm showed that the B cell, T cell CD4+, Neutrophil and Myeloid dendritic cells in HLA-G high-expression group were significantly increased ($p < 0.001$). CIBERSORT algorithm showed that T cell CD8+, T cell CD4+ memory activated and Macrophage M1 were significantly increased in HLA-G high expression group ($p < 0.001$) (figure 9A-B), and the heat map visualized the percentage of abundance of tumor-infiltrating immune cells in each sample of low and high HLA-G group (figure 9C).

Correlation analysis of HLA-G expression with infiltrating immune cells in BLCA. (A-B) The infiltrating levels of immune cells in high and low HLA-G expression groups in BLCA patients. (C) The heat map visualized the percentage abundance of tumor-infiltrating immune cells in each sample. * $p < 0.05$, ** $p < 0.01$, and *** $p < 0.001$.

Correlation analysis of biomarkers between HLA-G and tumor immune infiltrating cells in BLCA TIMER 2.0 database was used to study the correlation between HLA-G in BLCA and biomarkers of tumor immune infiltrating cells, and the results showed that HLA-G was positively correlated with most biomarkers of tumor immune infiltrating cells with significant difference ($P < 0.05$). This further proves that HLA-G is significantly correlated with immune-infiltrating cells in bladder cancer (table 2).

TABLE 2 Correlation analysis between HLA-G and related genes and markers of immune cells in Tumor Immune Estimation Resource (TIMER2.0).

Cell type	Gene marker	None		Purity	
		Cor	P	Cor	P
B cell	CD19	0.205	***	0.060	0.249
	CD20(KRT20)	-0.224	***	-0.190	***
	CD38	0.488	***	0.363	***
CD8+ T cell	CD8A	0.499	***	0.411	***
	CD8B	0.440	***	0.366	***
Tfh	BCL6	-0.069	0.164	-0.042	0.420
	ICOS	0.462	***	0.359	***
	CXCR5	0.253	***	0.095	0.070
Th1	T-bet (TBX21)	0.428	***	0.328	***
	STAT4	0.425	***	0.334	***
	IL12RB2	0.420	***	0.351	***
	WSX1(IL27RA)	0.304	***	0.190	***
	STAT1	0.531	***	0.479	***
	IFN- γ (IFNG)	0.451	***	0.363	***
	TNF- α (TNF)	0.245	***	0.175	**
Th2	GATA3	-0.155	**	-0.088	0.191
	CCR3	0.097	0.051	0.037	0.474
	STAT6	0.017	0.727	0.070	0.177
	STAT5A	0.305	***	0.241	***
Th9	TGFB2	0.207	***	0.146	**
	IRF4	0.376	***	0.241	***
	PU.1(SPI1)	0.421	***	0.293	***
Th17	STAT3	0.324	***	0.282	***
	IL21R	0.466	***	0.366	***
	IL23R	0.133	**	0.115	*
	IL17A	0.234	***	0.234	***
Th22	CCR10	0.024	0.626	-0.024	0.641
	AHR	-0.096	0.053	-0.053	0.314
Treg	FOXP3	0.414	***	0.303	***
	CD25(IL2RA)	0.416	***	0.293	***
	CCR8	0.358	***	0.247	***
T cell exhaustion	PD-1 (PDCD1)	0.505	***	0.412	***
	CTLA4	0.454	***	0.351	***
	LAG3	0.482	***	0.394	***
	TIM-3 (HAVCR2)	0.452	***	0.341	***
Macrophage	CD68	0.388	***	0.293	***
	CD11b (ITGAM)	0.391	***	0.248	***
M1	iNOS (NOS2)	0.241	***	0.198	***
	IRF5	-0.088	0.075	-0.104	*
	COX2(P1GS2)	0.100	*	0.064	0.221
M2	CD16(FCGR3B)	0.212	***	0.096	0.067
	ARG1	-0.122	*	-0.121	*
	MRC1	0.392	***	0.213	***
	MSA4A	0.392	***	0.253	***
TAM	CCL2	0.246	***	0.095	0.069
	CD80	0.411	***	0.295	***
	CD86	0.411	***	0.287	***
	CCR5	0.482	***	0.379	***
Monocyte	CD14	0.408	***	0.283	***
	CD16(FCGR3B)	0.212	***	0.096	0.067
	CD115 (CSF1R)	0.428	***	0.310	***
Neutrophil	CD66b(CEACAM8)	-0.021	0.668	0.038	0.462
	CD15(FUT4)	0.223	***	0.163	**
	CD11b (ITGAM)	0.391	***	0.248	***
Natural killer cell	XCL1	0.053	0.289	0.063	0.231
	CD7	0.473	***	0.374	***
Dendritic cell	KIR3DL1	0.308	***	0.272	***
	CD1C	0.150	**	0.019	0.722
	CD141 (THBD)	0.069	0.161	0.019	0.721
	CD11c (ITGAX)	0.353	***	0.205	***

Cor, R value of Spearman's correlation; None, correlation without adjustment; Purity; correlation adjusted by purity. *p < 0.01; **p < 0.001; ***p < 0.0001.

The expression of HLA-G is associated with immunomodulators and chemokines in BLCA

Immunomodulator is an important substance that affects the function of immune system. This study showed that HLA-G expression was positively correlated with Immunoinhibitor, and P < 0.001 (Figure

11A). Meanwhile, we also found that HLA-G expression was closely related to immunestimulants and chemokines (figure 11B-D). These results suggest that HLA-G is closely involved in the regulation of immune interactions and may regulate tumor immune escape.

The expression of HLA-G is associated with immunomodulators and chemokines in BLCA. (A) Correlation between HLA-G expression and immunoinhibitors in BLCA available at TISIDB database. (B) Correlation between HLA-G expression and immunostimulators in BLCA available at TISIDB database. (C) Correlation between HLA-G expression and chemokines in BLCA available at TISIDB database. (D) Correlation between HLA-G expression and chemokine receptors in BLCA available at TISIDB database. Color images are available online.

Discussion

Bladder cancer is one of the top ten tumors with high morbidity and mortality. In-depth study of bladder tumor immune microenvironment and search for effective biomarkers that can be used to identify and predict the survival of bladder patients can improve the prognosis of bladder cancer patients. In cancer, although cell senescence can be used as a mechanism to inhibit tumor development, SASP produced by cell senescence can promote the treatment resistance and recurrence of cancer [10]. Senescent cells often play a deleterious role in TME, especially those in SASP in advanced cancer [11]. Therefore, SASP plays an important role in tumor immune microenvironment. Here we distinguished two independent subtypes with differential clinical features, prognoses, PD-L1 expression, and TIME via consensus clustering for selected SASP-related genes. Among these, HLA-G was identified as the potential immune infiltration-related SASP-related genes.

In recent years, the concept of precision medicine has promoted the subcomponent type of a single research object. Different subgroups have different pathogenic mechanisms and clinical prognostic characteristics, which can subdivide highly heterogeneous cancers into more accurate subtypes for individualized treatment. Based on gene expression levels, data were divided into two subgroups using R's ConsensusClusterPlus package. Principal component analysis showed a separation between subgroup1 and subgroup2[13]. Overall survival analysis indicated that survival duration of subgroup1 significantly improved, suggesting that survival time correlated with comprehensive expression level of SASP-related genes.

The LASSO algorithm analyzes all independent variables simultaneously and selects the most influential variables [14]. According to LASSO Cox analysis, 12 of 18 genes (MAPK3, SRC, CD36, VEGFA, IL4, HLA-G, SPINK1, IGF1, EGFR, GATA4, NFKB1, PRKG1) were identified as prognostic factors for BLCA. The predictive power of SASP-related genes on BLCA prognosis was evaluated by the ROC curve. The results demonstrated that SASP-related genes were involved in the survival of BLCA. We also analyzed the correlation between the prognostic model constructed by SASP-related genes and immune infiltration. The results of TIMER method showed that B cell, T cell CD4+, T cell CD8+, Neutrophil, Macrophage and Myeloid dendritic cell was positively correlated with SASP-related genes prognosis model (Fig. 7A). SASP-

related genes prognosis model was positively correlated with cytotoxicity score, NK cell, B cell, Macrophage/Monocyte, Myeloid dendritic cell, Endothelial cell by MCPCOUNTER method.

In addition, TIMER2.0 and TISIDB databases were used to evaluate the correlation between HLA-G expression and biomarkers of tumor immune infiltrating cells, immunostimulants, immunosuppressants, chemokines and receptors in bladder cancer, and the results showed that HLA-G expression was significantly correlated with all of them. This further proves that HLA-G expression plays an important role in immune invasion in bladder cancer. In this study, we conducted a comprehensive bioinformatics investigation to systematically analyze the clinical significance and expression level of SASP-related genes in BLCA. In addition, our data suggest that HLA-G expression is closely related to the degree of infiltration of different immune cells, immune stimulants, immunosuppressants, chemokines and receptors in BLCA. Therefore, our study provides insight into the key functions of SASP-related genes, of course, this study has some limitations. The model we built is based on online database, without validation from independent cohorts, so we need more studies to verify our conclusions.

Conclusion

This study systematically analyzed the expression profile of SASP-related genes in BLCA and its correlation with prognosis, PD-L1 and its role in TIME. Favorable prognostic biomarkers for BLCA were found by constructing prognostic model. In conclusion, our study provides important evidence for future research on the role of SASP in BLCA.

Abbreviations

TCGA The cancer genome atlas

SASP senescence-associated secretory phenotype

BLCA Bladder Urothelial Carcinoma

CI confidence interval

HR hazard ratio

TIME Tumor Immune Estimation

Declarations

Ethical approval and consent to participate

Not applicable.

Consent for publish

Not applicable.

Authors' contributions

Wang Yaxuan wrote the full text, and Xiaolin Wang and HaiXia Zhu was responsible for reviewing it.

Funding

This study was supported by the Scientific research project of Jiangsu Provincial Health Commission (M2021005).

Acknowledgements

Not applicable.

Competing interests

The authors declare that they have no competing interests.

Availability of data and materials

The datasets analyzed during the present study are available from The Cancer Genome Atlas (TCGA) database (<https://portal.gdc.cancer.gov/>) GenesCords (<https://www.genecards.org/>) STRING (<https://cn.string-db.org/>), TIMER2.0 (<http://timer.cistrome.org/>), and TISIDB (<http://cis.hku.hk/TISIDB/index.php>).

References

1. Shi Z, Cai W, Feng X, et al. Radiomics Analysis of Gd-EOB-DTPA Enhanced Hepatic MRI for Assessment of Functional Liver Reserve. *Acad Radiol.* 2022;29(2):213-218.
2. Sung H, Ferlay J, Siegel RL, et al. Global Cancer Statistics 2020: GLOBOCAN Estimates of Incidence and Mortality Worldwide for 36 Cancers in 185 Countries. *CA Cancer J Clin.* 2021 May;71(3):209-249.
3. Kirkali Z, Chan T, Manoharan M, et al. Bladder cancer: epidemiology, staging and grading, and diagnosis. *Urology.* 2005;66(6 Suppl 1):4-34.
4. Farina MS, Lundgren KT, Bellmunt J. Immunotherapy in urothelial cancer: recent results and future perspectives. *Drugs.* 2017;77(10):1077-1089.
5. Crispen PL, Kusmartsev S. Mechanisms of immune evasion in bladder cancer. *Cancer Immunol Immun.* 2019;69(1):3-14.
6. Wu Q, Li B, Liu L, et al. Centrosome dysfunction: a link between senescence and tumor immunity. *Signal Transduct Target Ther.* 2020 Jun 30;5(1):107.
7. Kumar V, Gabilovich DI. Hypoxia-inducible factors in regulation of immune responses in tumour microenvironment. *Immunology.* 2014;143(4):512-519.

8. Wang Z, Wang X, Xu Y, et al. Mutations of PI3K-AKT-mTOR pathway as predictors for immune cell infiltration and immunotherapy efficacy in dMMR/MSI-H gastric adenocarcinoma. *BMC Med.* 2022;20(1):133.
9. Noviello D, Mager R, Roda G, et al. The IL23-IL17 Immune Axis in the Treatment of Ulcerative Colitis: Successes, Defeats, and Ongoing Challenges. *Front Immunol.* 2021, 17(12):611256.
10. Childs BG, Gluscevic M, Baker DJ, et al. Senescent cells: an emerging target for diseases of ageing. *Nat Rev Drug Discov.* 2017;16(10):718-735.
11. Takasugi M, Yoshida Y, Hara E, et al. The role of cellular senescence and SASP in tumour microenvironment. *FEBS J.* 2022 Feb 2.
12. Zhang H, Ahearn TU, Lecarpentier J, et al. Genome-wide association study identifies 32 novel breast cancer susceptibility loci from overall and subtype-specific analyses. *Nat Genet.* 2020;52(6):572-581.
13. Liu J, Sun G, Pan S, et al. The Cancer Genome Atlas (TCGA) based m6A methylation-related genes predict prognosis in hepatocellular carcinoma. *Bioengineered.* 2020;11(1):759-768.
14. Friedman J, Hastie T, Tibshirani R. Regularization Paths for Generalized Linear Models via Coordinate Descent. *J Stat Softw.* 2010;33(1):1–22.

Figures

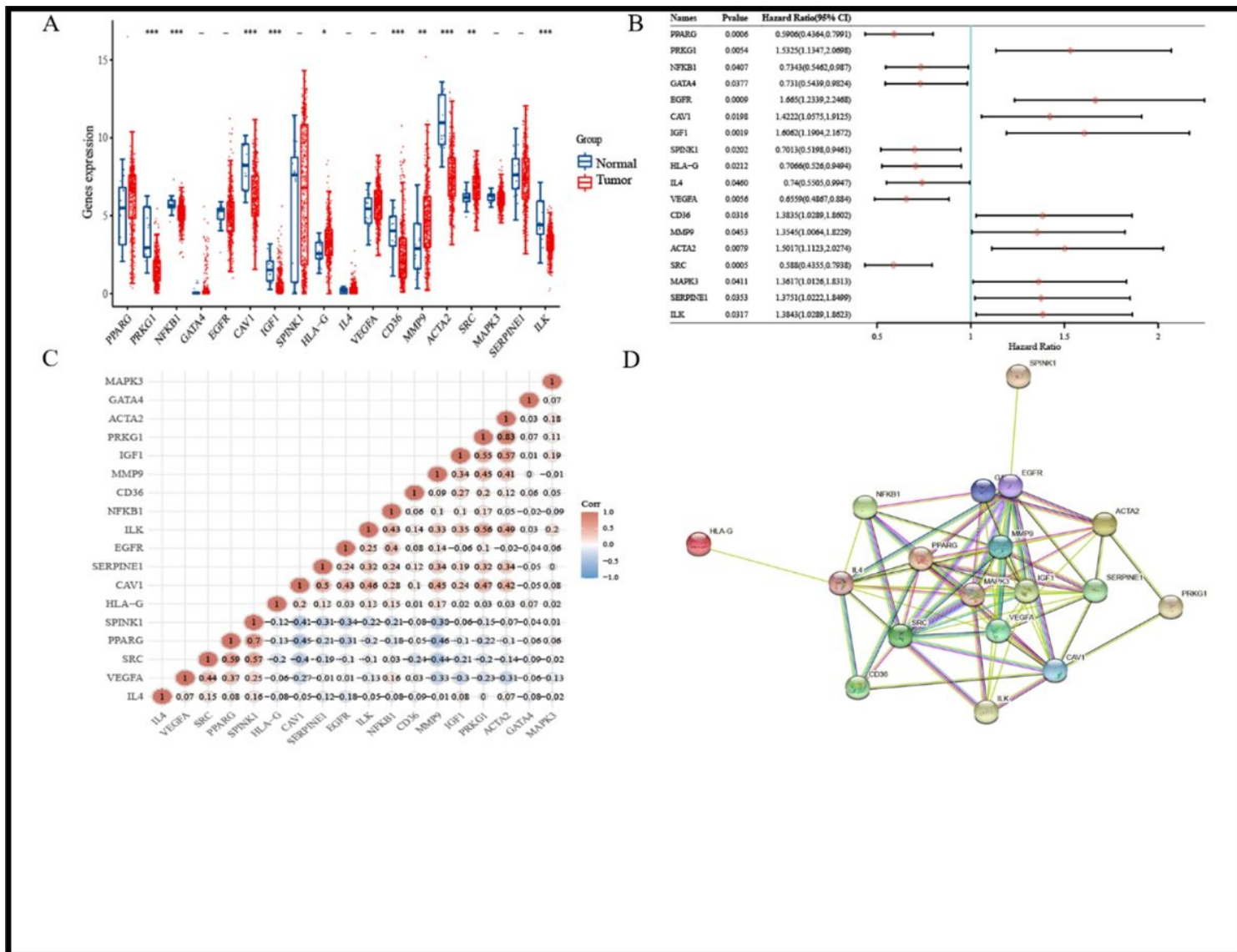


Figure 1

Figure legend not available with this version.

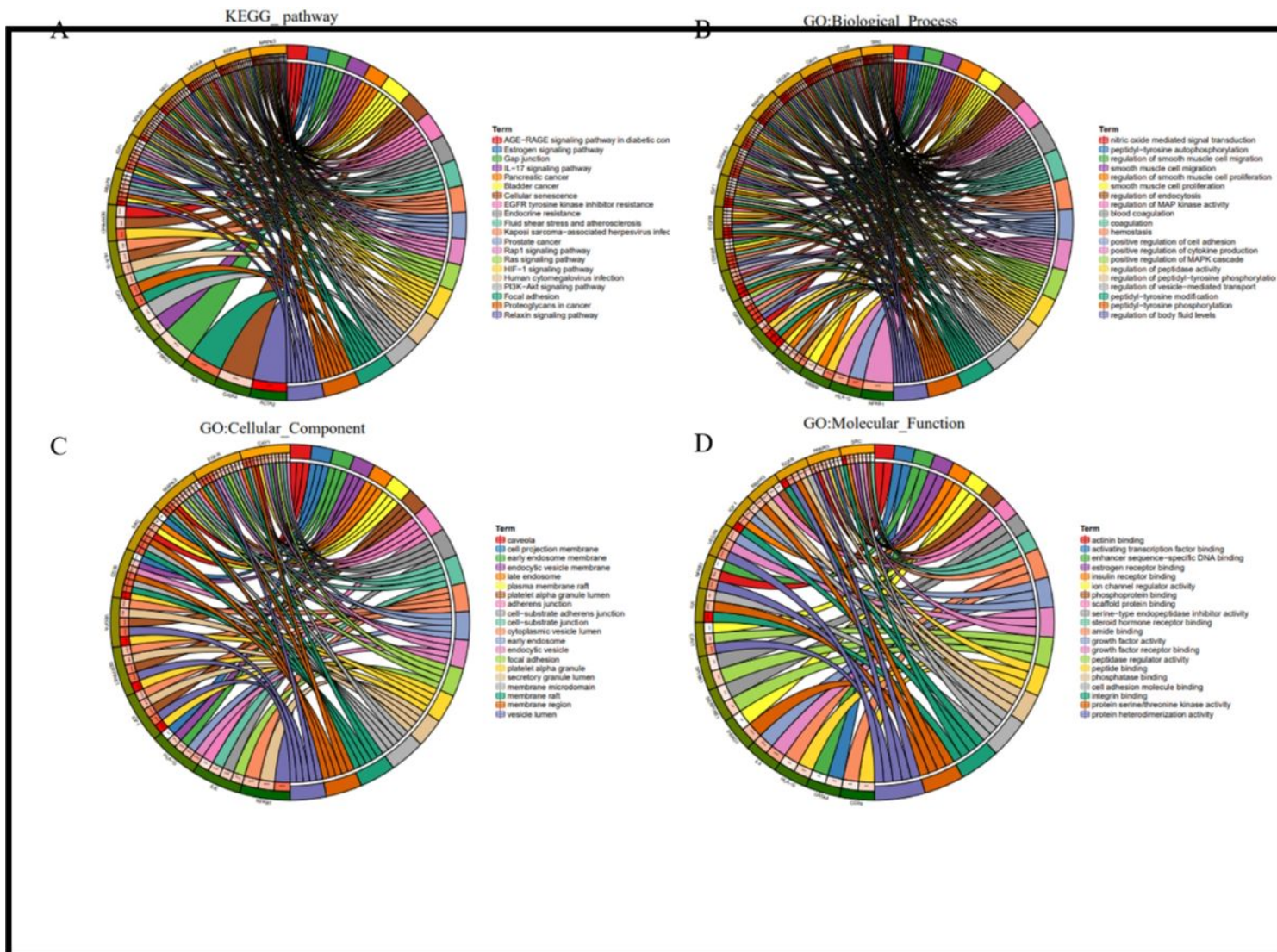


Figure 2

Figure legend not available with this version.

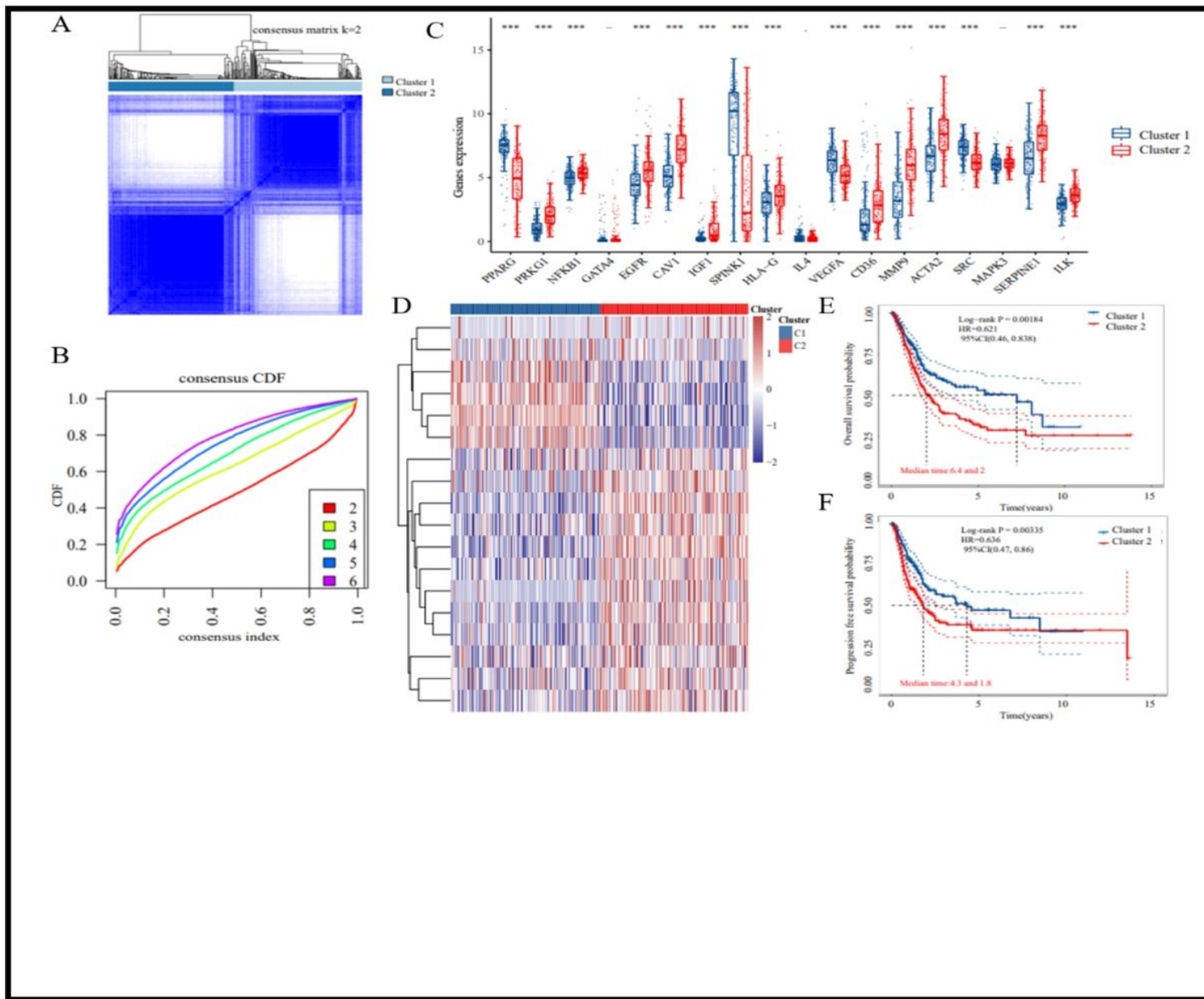


Figure 3

Figure legend not available with this version.

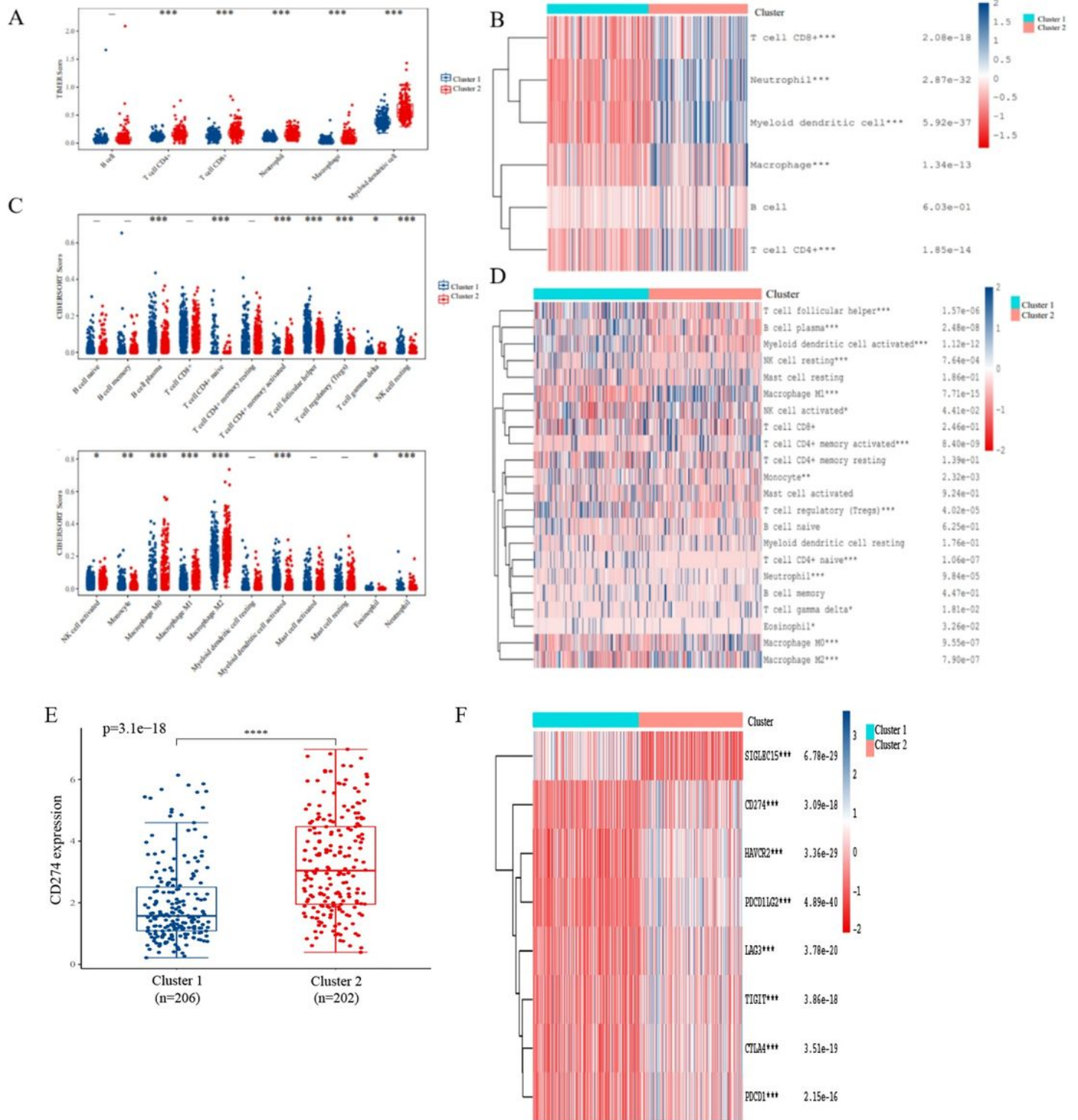


Figure 4

Figure legend not available with this version.

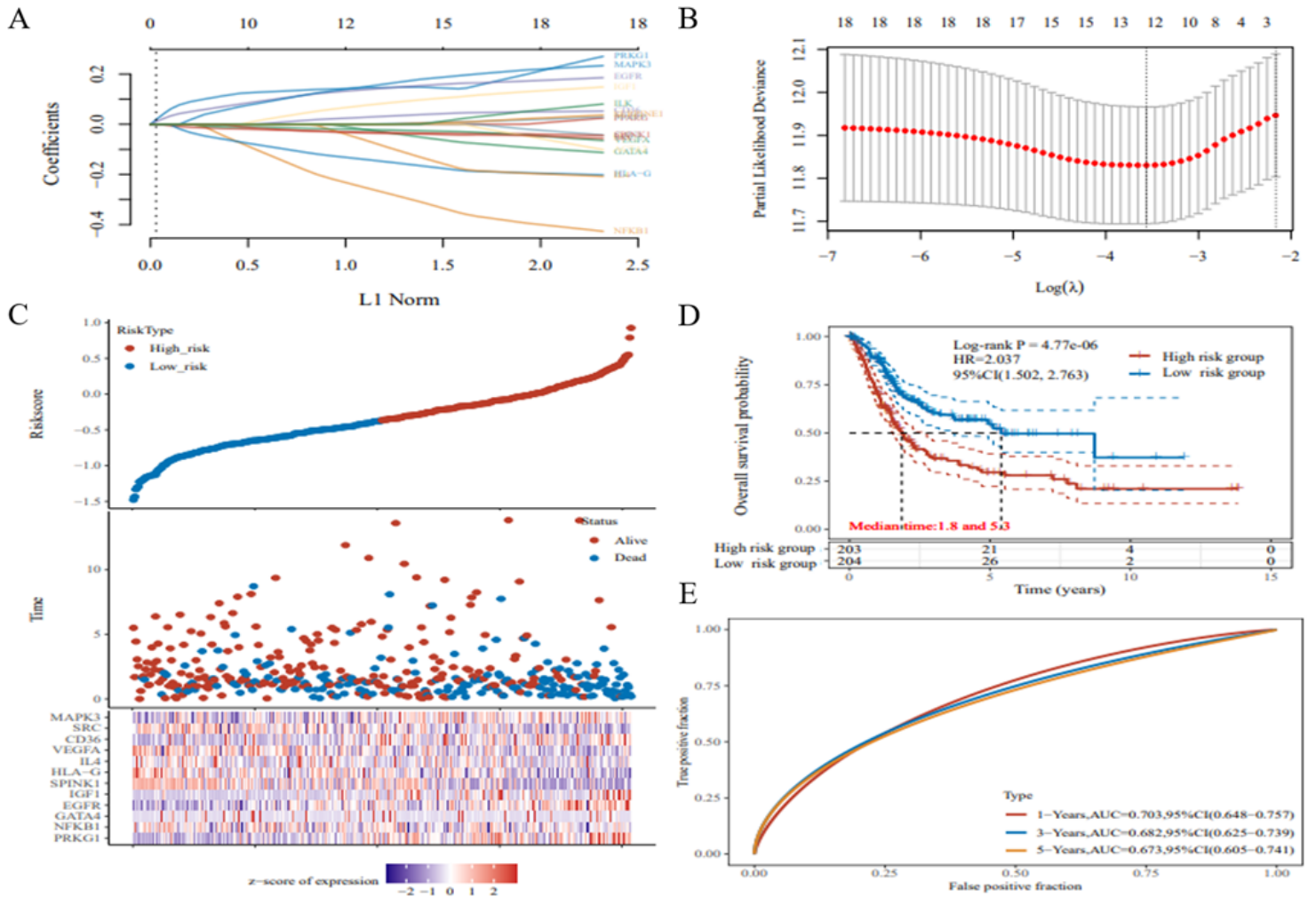


Figure 5

Figure legend not available with this version.

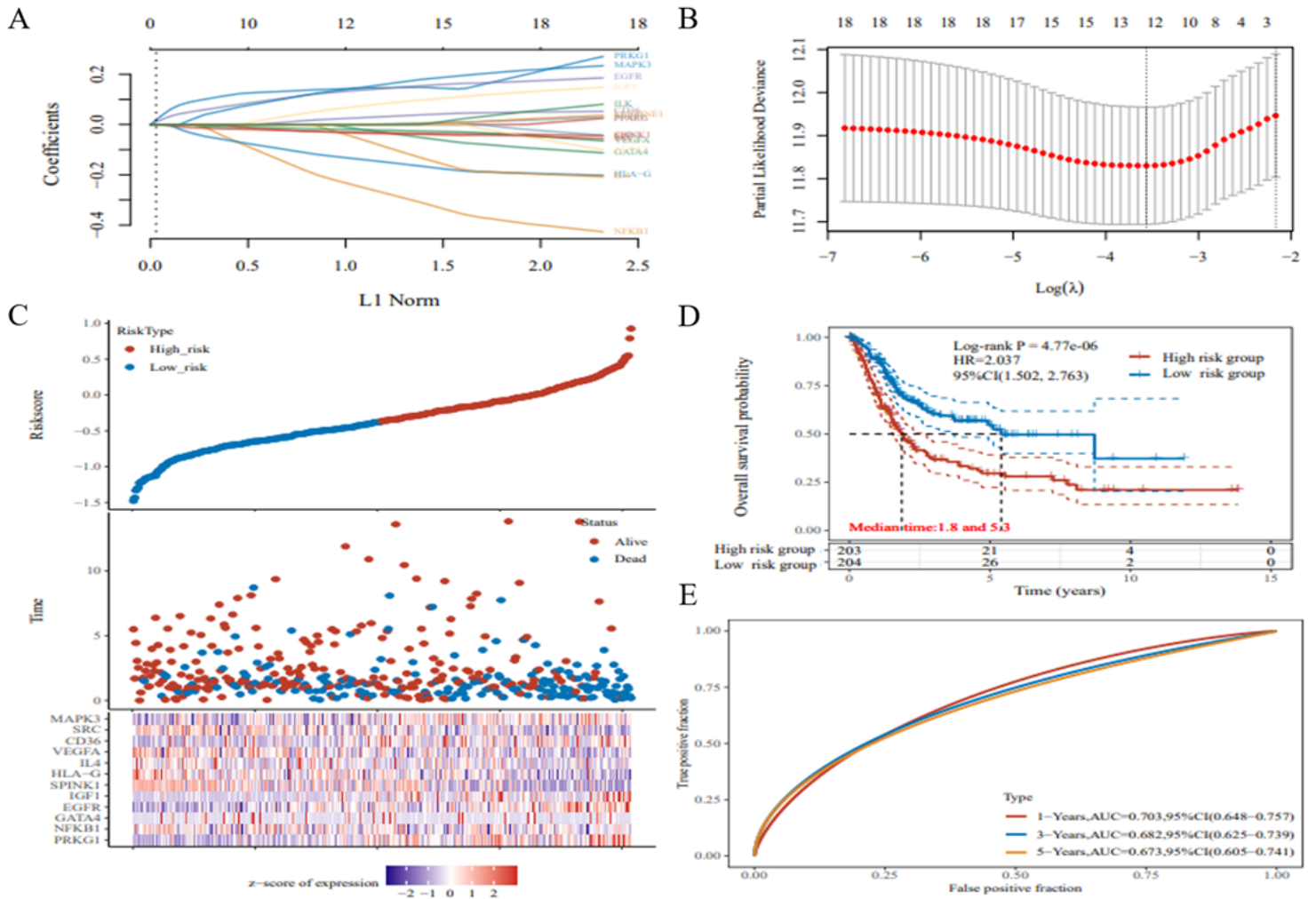


Figure 6

Figure legend not available with this version.

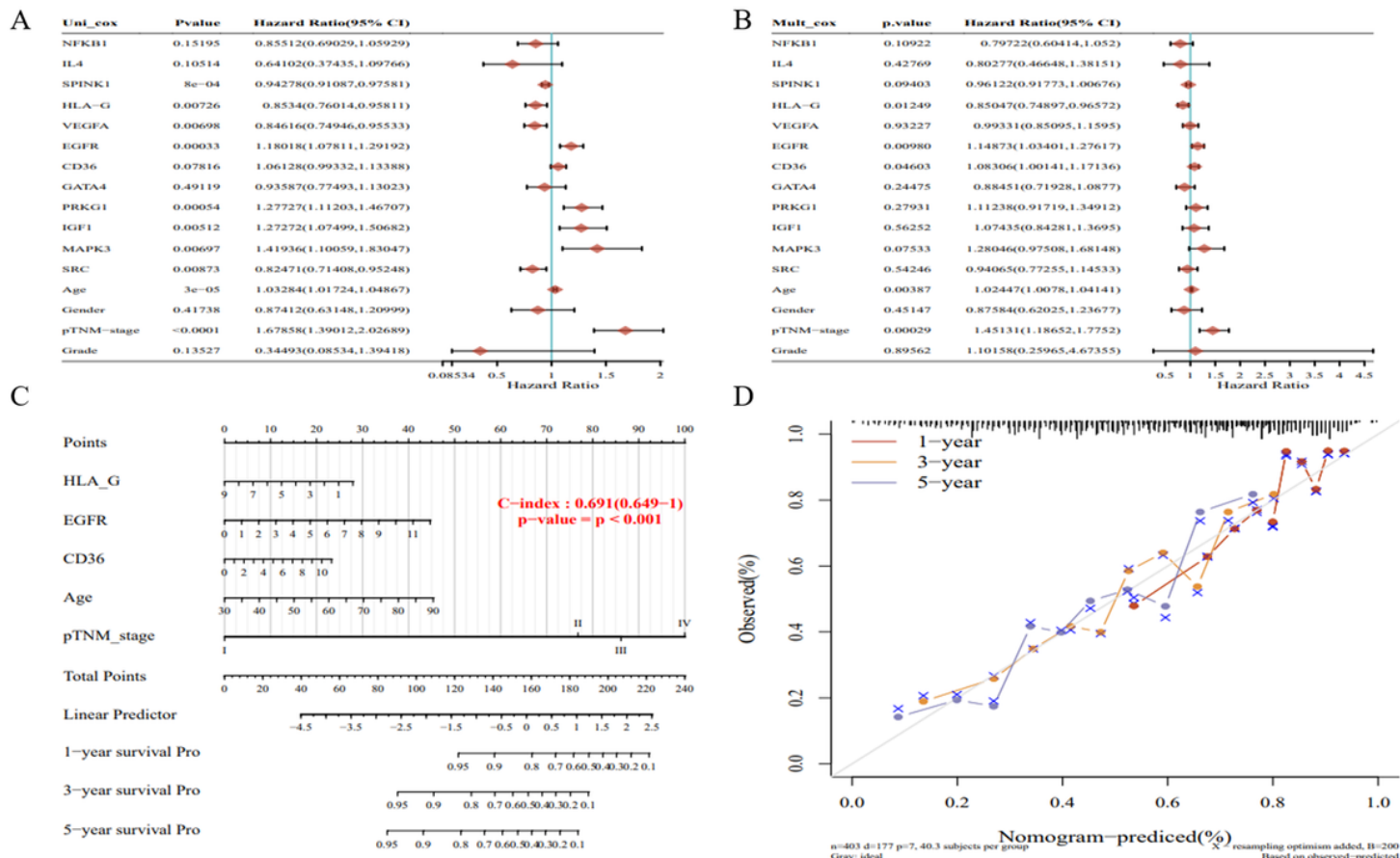


Figure 7

Figure legend not available with this version.

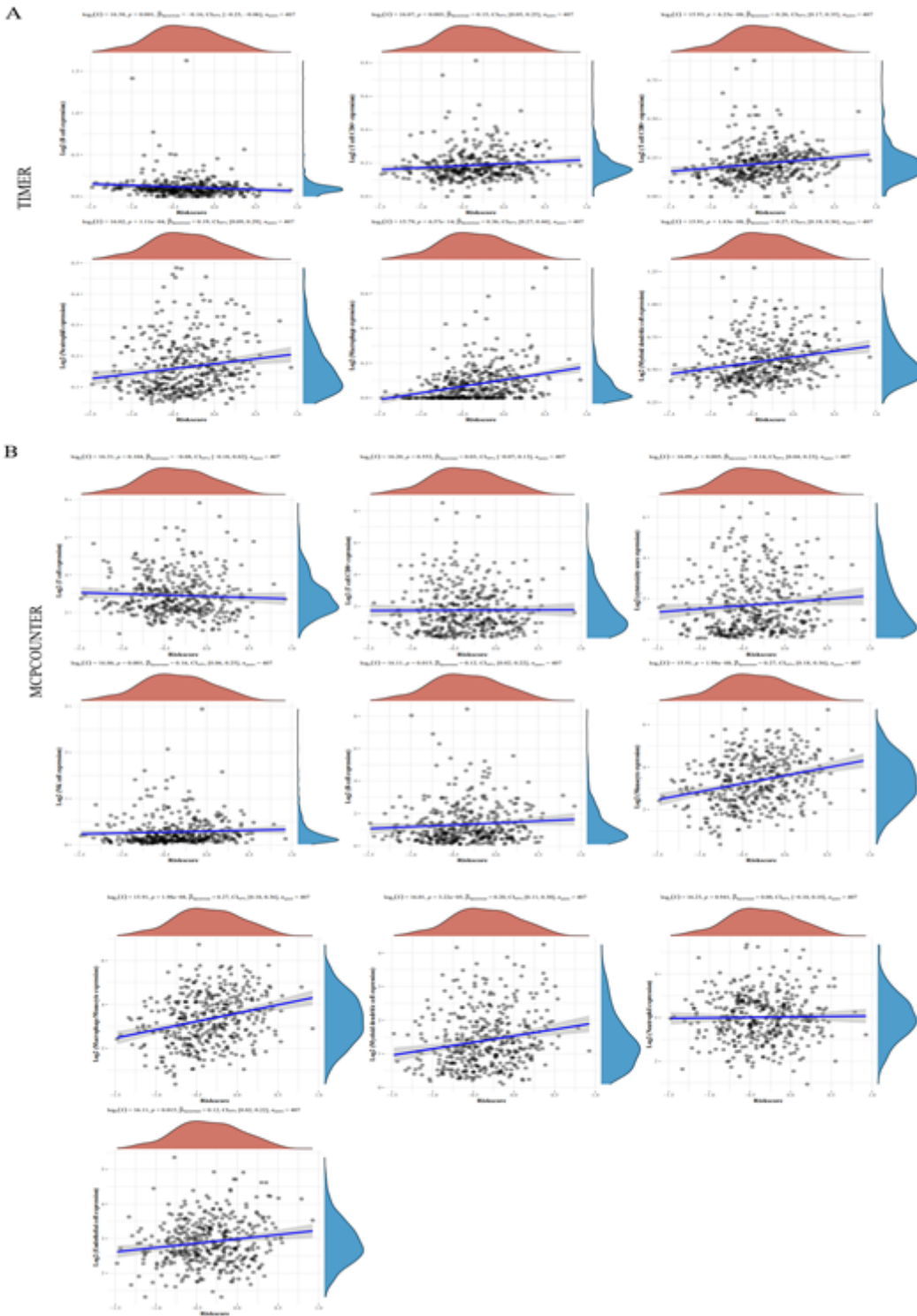


Figure 8

Figure legend not available with this version.

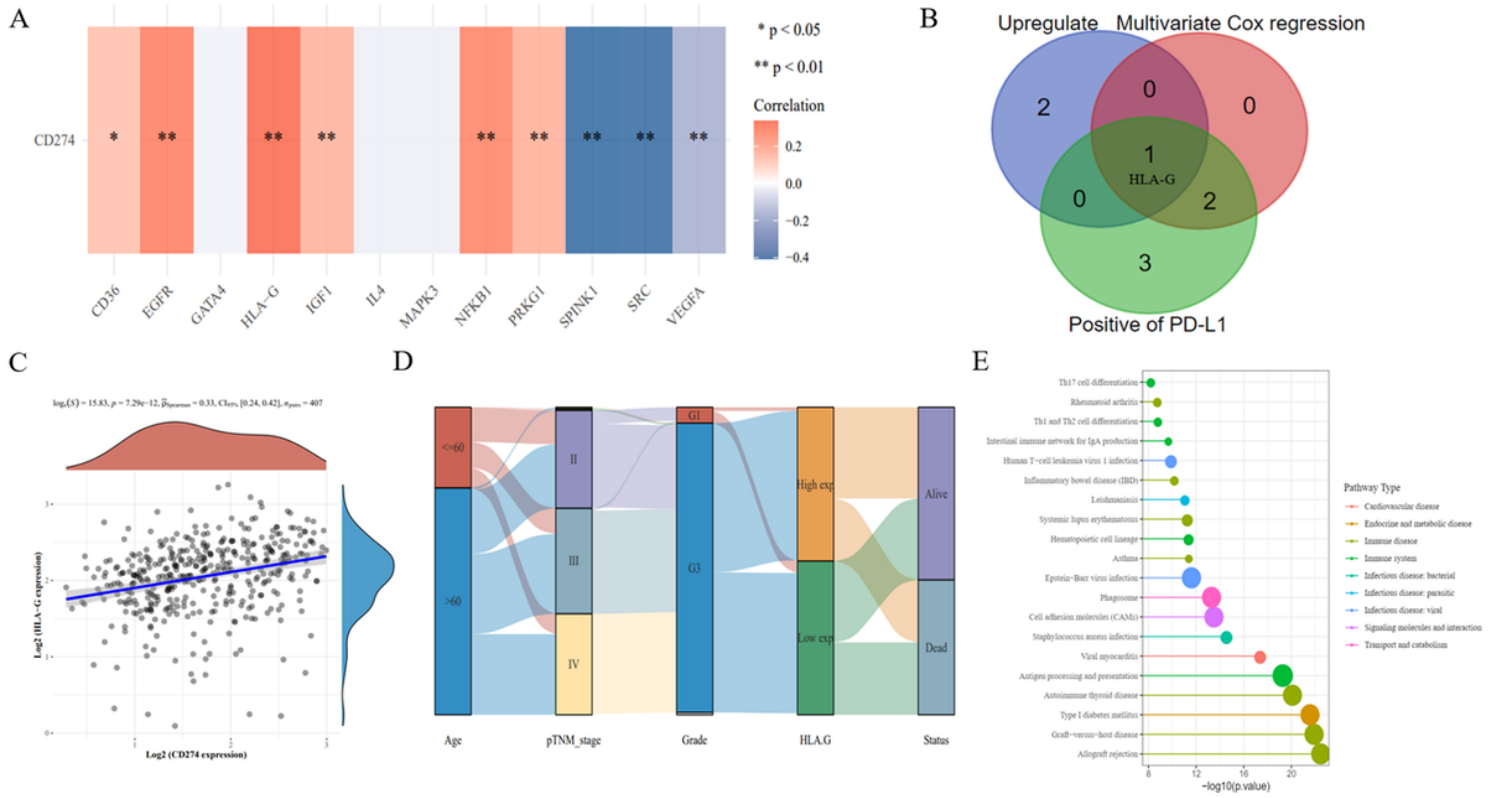


Figure 9

Figure legend not available with this version.

